AIP | Applied Physics Letters

Temperature stable and fatigue resistant lead-free ceramics for actuators

Amir Khesro, Dawei Wang, Fayaz Hussain, Derek C. Sinclair, Antonio Feteira, and Ian M. Reaney

Citation: Applied Physics Letters **109**, 142907 (2016); doi: 10.1063/1.4964411
View online: http://dx.doi.org/10.1063/1.4964411
View Table of Contents: http://scitation.aip.org/content/aip/journal/apl/109/14?ver=pdfcov
Published by the AIP Publishing

Temperature stable and fatigue resistant lead-free ceramics for actuators

Amir Khesro,[1,a)] Dawei Wang,[1] Fayaz Hussain,[1] Derek C. Sinclair,[1] Antonio Feteira,[2] and Ian M. Reaney[1]
[1]*Functional Materials and Devices Lab, Department of Materials Science and Engineering, Sir Robert Hadfield Building, University of Sheffield, Sheffield S1 3JD, United Kingdom*
[2]*Materials and Engineering Research Institute, Sheffield Hallam University, Howard Street, Sheffield S1 1WB, United Kingdom*

(Received 4 August 2016; accepted 24 September 2016; published online 6 October 2016)

Lead-free ceramics with the composition $0.91K_{1/2}Bi_{1/2}TiO_3$–$0.09(0.82BiFeO_3$-$0.15NdFeO_3$-$0.03Nd_{2/3}TiO_3)$ were prepared using a conventional solid state, mixed oxide route. The ceramics exhibited a high strain of 0.16% at 6 kV mm^{-1}, stable from room temperature to 175 °C, with a variation of <10%. The materials were fabricated into multilayer structures by co-firing with Pt internal electrodes. The prototype multilayer actuator exhibited constant strains up to 300 °C with a variation of ~15%. The composition showed fatigue resistant behaviour in both monolithic and multilayer form after bipolar loading of 10^6 cycles. [http://dx.doi.org/10.1063/1.4964411]

A piezoelectric or electrostrictive actuator converts an electrical signal into a precisely controlled mechanical strain. The ability to control physical displacements with high precision is vital for applications such as cameras, phones, microscopes, fuel injectors, micro-pumps, ink cartridges, and medical instruments.[1] Many harsh environments including oil well drilling, aerospace, automobile, and power plant engines require technological devices capable of retaining functional properties at elevated temperatures.[2,3] $Pb(Zr,Ti)O_3$ (PZT)-based piezoelectric and $Pb(Mg_{1/3}Nb_{2/3})O_3$ (PMN)-based electrostrictive ceramics are most widely used in actuator devices due to their large electromechanical coupling coefficients.[4] Electromechanical strain in PMN-based ceramics is not stable in high temperature regimes due to the notable temperature dependence of polarization above the permittivity maximum.[5,6] In the case of piezoelectrics, electromechanical coupling is restricted by the Curie or depoling temperature (T_c and T_d, respectively), and functional properties are lost above these transitions. High temperature applications, therefore, require materials with both high T_c and T_d. Long term reliability is another important aspect for real world applications. Continuous electrical cycling can cause severe degradation in strain as evident from many studies on PZT-based piezoelectrics.[7–9]

Recent concern, however, is the amount of toxic lead used in both PZT- and PMN-based systems, giving rise to health and environment concerns over the use of these materials in actuators. Lead-free piezoelectric/electrostrictive materials are therefore required with properties at least comparable and most preferably exceeding those containing lead, especially in terms of temperature stability and fatigue resistance.

Over the last two decades, many lead-free systems have been investigated, among them $(K,Na)NbO_3$ (KNN)-based, $Na_{1/2}Bi_{1/2}TiO_3$ (NBT)-based, and $BaTiO_3$ (BT)-based systems are the most prominent.[10] All these ceramics have their own shortcoming inhibiting their use for high temperature applications. BT-based ceramics have a low T_c,[11] and KNN-based ceramics suffers from temperature sensitivity of the polymorphic phase boundaries.[12,13] NBT-based ceramics have a low T_d and require high driving fields, where self-heating becomes an issue.[14]

Less widely investigated than NBT, KNN, and BT, $K_{1/2}Bi_{1/2}TiO_3$ (KBT) has also shown promise as a potential precursor for the development of lead-free piezoelectrics. KBT has the perovskite structure with tetragonal symmetry at room temperature (RT) and a T_c of 380 °C.[15,16] The piezoelectric properties of KBT are moderate ($d_{33} = 69$ pC/N and strain 0.1% at 8 kV/mm) for hot pressed ceramics.[15] Doping with $BiFeO_3$ (BF) improves the piezoelectric properties of KBT,[17–20] and Morozov *et. al.*[19] reported a high RT strain performance of 250 pm/V. However, the strain showed an increase by around 48% when the temperature was increased from RT to 100 °C.

BF has a high T_c of 830 °C,[21] which is very attractive for high temperature applications, but BF is usually very conductive, and high fields cannot be applied to access the electromechanical properties.[22] The high conductivity of BF has been attributed to the presence of oxygen vacancies formed due to the reduction of Fe^{3+} to Fe^{2+} during processing.[23] Recently, Khesro *et al.*[24] showed that electrically homogenous ceramics with activation energy >1 eV could be obtained in the series $(0.95\text{-}x)BiFeO_3$-$xLaFeO_3$-$0.05La_{2/3}TiO_3$ and that these compositions were either ferroelectric with *R*3*c* symmetry or antiferroelectric with *Pbam* symmetry depending on the value of *x*. Further research by the present authors showed similar structural trends as a function of *x* for Nd containing analogues of this solid solution, and it was concluded that $(1\text{-}x\text{-}y)BiFeO_3$-$xREFeO_3$-$yRE_{2/3}TiO_3$ (RE = rare earth) compositions might provide a low dielectric loss end-member in solid solution with KBT for the fabrication of lead-free actuator materials.

a)E-mail: amir.khesro@sheffield.ac.uk

Based on this concept, we comprehensively studied the solid solution $(1\text{-}x)K_{1/2}Bi_{1/2}TiO_3\text{-}x(0.82BiFeO_3\text{-}0.15NdFeO_3\text{-}0.03Nd_{2/3}TiO_3)$. The composition $0.82BiFeO_3\text{-}0.15NdFeO_3\text{-}0.03Nd_{2/3}TiO_3$ was preferred as an end member with KBT because of its antiferroelectric *Pbam* symmetry similar to $PbZrO_3$. Optimum properties (~0.16% strain at 6 kV mm^{-1}) were obtained at $x = 0.09$, hereafter abbreviated as KBNFT9. The induced strain was temperature stable up to 175 °C with a variation of strain (ΔS) < 10% and fatigue resistant up to 10^6 cycles at 5 kV mm^{-1}. It should be noted that higher temperature strain measurements could not be performed on monolithic ceramics due to safety restrictions on the measuring equipment. In addition to temperature-stable, fatigue-resistant monolithic ceramics, multilayer actuators (MLA) were fabricated using Pt internal electrodes, which yielded ~2 μm displacement at 6 kV mm^{-1}, stable up to 300 °C ($\Delta S \sim 15\%$). The MLA also exhibited fatigue resistant behaviour up to 10^6 cycles at 5 kV mm^{-1} bipolar field.

KBNFT9 ceramics were prepared by a conventional solid state oxide route, and MLAs were fabricated using the tape casting technique. The details of both processes can be found elsewhere.[24,25] However, it is useful to note that ceramics both in monolithic and multilayer form were sintered at 1090 °C for 2 h.

For X-ray powder diffraction (XRD) measurements, sintered pellets were crushed and then annealed at 500 °C overnight to reduce the effect of mechanical strain produced during grinding. XRD was performed using a Siemens D5000 diffractometer with CuKα. Optical micrographs were recorded using a Polyvar Met optical microscope. Ceramic microstructures were studied using an FEI Inspect F, Scanning Electron Microscope (SEM). For electrical measurements, the pellets were ground and polished to a thickness of ~0.7 mm and then electroded on both sides using gold paste. Multilayers were silver painted to form termination electrodes. The LCR measurements were carried out at fixed frequencies of 1, 10, 100, and 250 kHz from RT to 550 °C using a precision Agilent 4184A LCR meter. Polarization (P) and bipolar strain (S) vs. electric field (E) were measured using an aix-ACCT (PES) ferroelectric test unit.

A RT XRD pattern of KBNFT9 annealed crushed pellets is shown in Figure 1(a). All peaks are attributed to a single perovskite structured phase, similar to the pseudocubic structure reported in KBT-BF systems.[17–20] Figure 1(b) is a secondary electron SEM image of KBNFT9 showing a dense microstructure of cuboid grains with an average size of <1 μm.

Relative permittivity (ε_r) and tan δ plotted against temperature for KBNFT9 are presented in Figure 1(c). ε_r is strongly frequency dependent below the peak maximum in permittivity (T_m). The overall behaviour is similar to that of relaxor ferroelectrics, but it is important to note that tan δ decreases to <2% at higher temperatures, suggesting that the relatively high losses at RT arise primarily from the dielectric relaxation rather than long range conduction. Pure KBT has been shown to possess weak relaxor behaviour attributed to compositional disorder of K^+ and Bi^{3+} cations on the A-site.[26,27] The formation of a solution with $0.82BiFeO_3\text{-}0.15NdFeO_3\text{-}0.03Nd_{2/3}TiO_3$ has significantly increased peak broadening and frequency dispersion indicating an enhancement in relaxation.

RT strain-field (S-E) and polarization-field (P-E) loops for KBNFT9 are shown in Figure 1(d). P-E loop was not saturated at 6 kV mm^{-1}, with a low remanent polarization (P_r) of ~9 μC/cm^2. The slim P-E loop and low P_r is consistent with the maximum broad permittivity (Figure 1(c)) and indicative of dominant relaxor-like behaviour. Moreover, the bipolar S-E loop shows a very low ~0.01% of negative strain suggesting the absence of long range ferroelectric order. KBNFT9 exhibits a high positive RT strain of ~0.16% at 6 kV mm^{-1}, which appears predominantly electrostrictive. The electrostrictive coefficient (Q_{33}) is 0.023 m^4 C^{-2}, similar to PMN-based ceramics,[28] and was calculated using

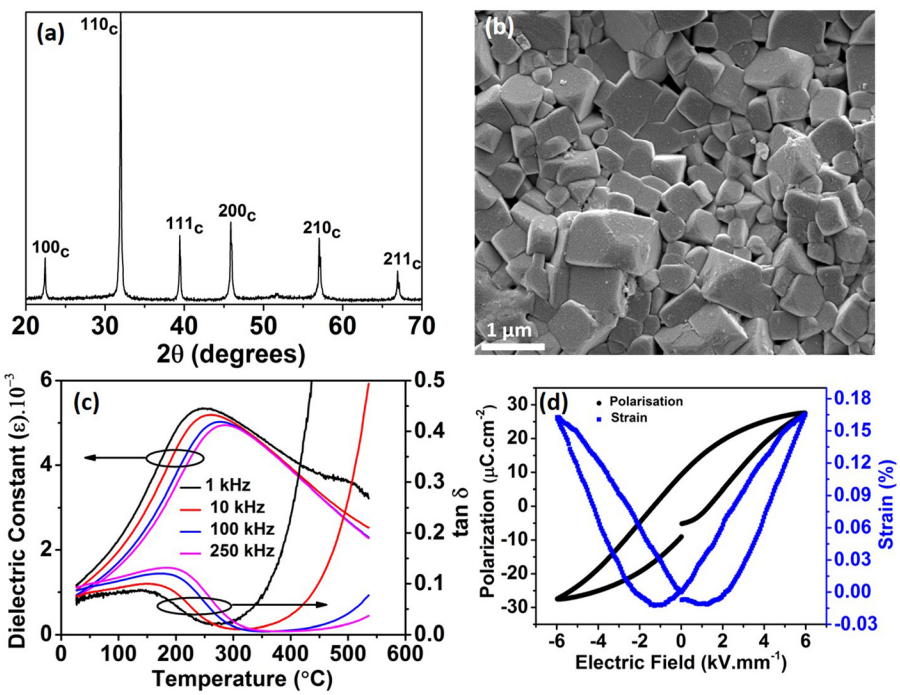

FIG. 1. (a) XRD pattern of KBNFT9 at RT; (b) the ceramic microstructure of KBNFT9; (c) permittivity and tan δ versus temperature for KBNFT9 ceramics; (d) P-E and S-E loops for KBNFT9 bulk ceramics at RT and at a frequency of 1 Hz.

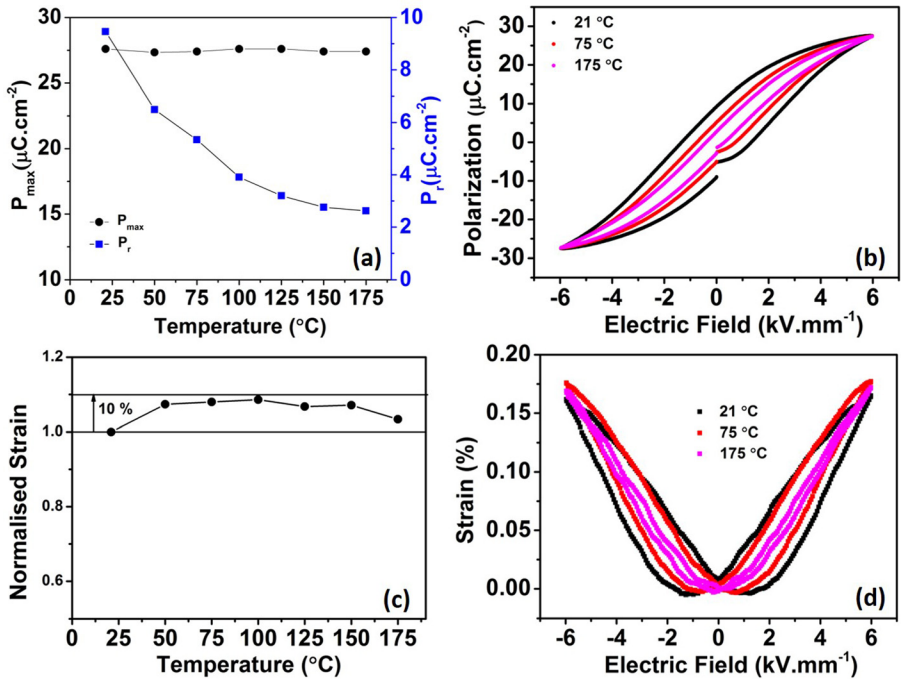

FIG. 2. (a) Maximum and remanent polarization versus temperature for KBNFT9 bulk ceramics; (b) P-E loops for KBNFT9 bulk ceramics at different temperatures; (c) normalised bipolar strain versus temperature for KBNFT9 bulk ceramics; and (d) S-E loops for KBNFT9 bulk ceramics at different temperatures.

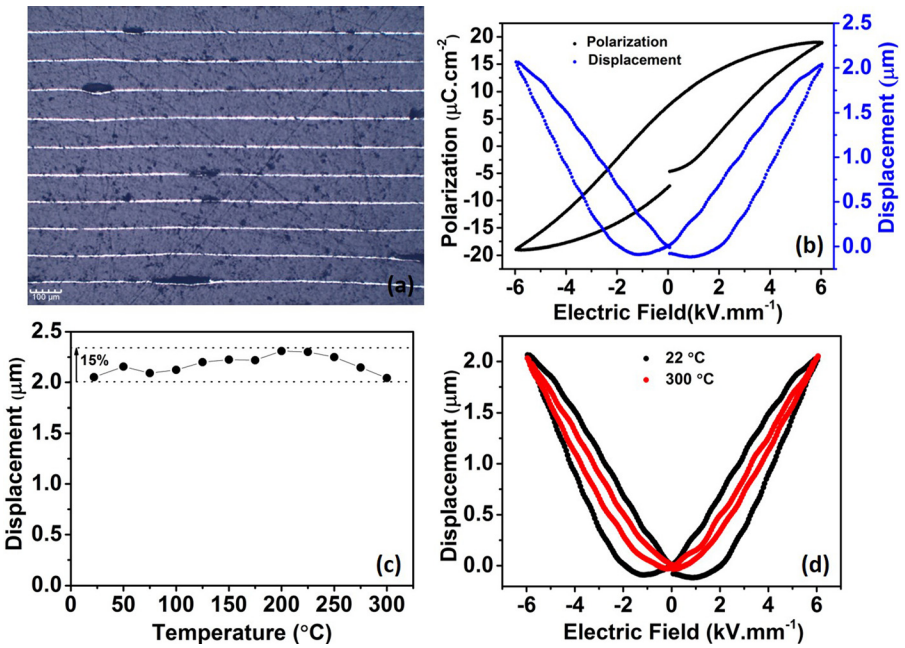

FIG. 3. (a) Optical image of a KBNFT9 MLA cross section; (b) P-E and S-E loops for KBNFT9 MLA at RT and at a frequency of 1 Hz; (c) displacement versus temperature for KBNFT9 MLA; and (d) S-E loops for KBNFT9 MLA at 22 and 300 °C.

$$S_3 = Q_{33}P_3^2, \quad (1)$$

where S_3 and P_3 are the strain and polarization in the direction of poling, respectively.

The maximum polarization (P_{max}) and P_r as a function of temperature for bulk KBNFT9 ceramics is shown in Figure 2(a). P_r decreases with the increasing temperature from 9.46 μC cm^{-2} at RT to 2.62 μC cm^{-2} at 175 °C resulting in slimmer loops as shown in Figure 2(b), but P_{max} exhibits negligible temperature dependence. From Equation (1), electrostrictive strain is directly proportional to the square of polarization. A temperature stable P_{max}, as shown in Figure 2(a), should therefore lead to temperature stable electromechanical strain. S-E loops at different temperatures for bulk KBNFT9 ceramics are shown in Figure 2(d). The strain exhibited by KBNFT9 is broadly insensitive ($\Delta S \sim 10\%$) to temperature between RT and 175 °C, as shown in Figure 2(c).

Owing to its promising properties in thick bulk samples, KBNFT9 was co-fired with platinum internal electrodes to

TABLE I. The temperature stability of KBNFT9 vs. leading lead based materials.

Material	Temperature range (°C)	Variation in strain (%)	References
0.9PMN-0.1PT	RT-70	>40	6
PZT-5H	RT-80	~40	30
PIC 151	RT-170	20	31
PZT 4	RT-160	15	29
KBNFT9	RT-300	15	This work

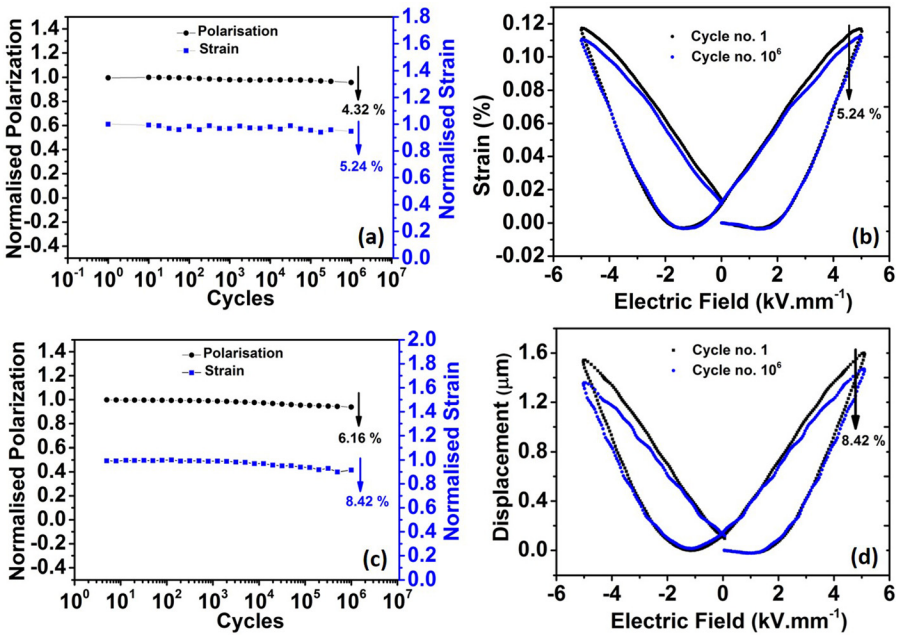

FIG. 4. (a) Polarization and strain for bulk KBNFT9 ceramics as a function of switching cycle; (b) S-E loops for KBNFT9 bulk ceramics at 1st and millionth cycle at 10 Hz; (c) polarization and strain for a KBNFT9 MLA as a function of switching cycle; and (d) comparison of S-E loops for KBNFT9 MLA at 1st and millionth cycle at 5 Hz.

form MLAs consisting of 10 active layers, as shown in Figure 3(a). The thickness of each sintered layer was ~83 μm, and the active area of each electrode was ~31.36 mm^2. The S-E and P-E loops of MLA at RT are shown in Figure 3(b). The MLA yielded a strain of ~2 μm at 498 V (6 kV mm^{-1}) demonstrating that KBNFT9 can be processed into a MLA without significant loss of performance at RT. More importantly, the MLA showed a broadly temperature insensitive strain up to 300 °C, as shown in Figure 3(c). A comparison of strain at RT and 300 °C is shown in Figure 3(d). KBNFT9 requires a higher field of 6 kV mm^{-1} for achieving a strain of ~0.16% as compared to PZT-based materials, e.g., PZT4 requires a field of 2 kV mm^{-1} to achieve a strain of ~0.14%.[29] However, the temperature stability in KBNFT9 is by far better than commercial lead-based ceramics. A comparison of KBNFT9 with commercially used lead-based materials is summarized in Table I. The values in Table I are taken from figures in the respective references.

To study the fatigue behaviour, KBNFT9 bulk ceramics were exposed to a bipolar loading of 5 kV mm^{-1} (~3E$_c$) for 10^6 cycles at a frequency of 10 Hz. Fatigue resistant behaviour is observed as shown in Figures 4(a) and 4(b) with the bipolar strain decreasing by <6% and P_{max} by <5% after 10^6 bipolar cycles. Similar to bulk samples, the prototype MLA also showed fatigue resistant properties, and only <9% of polarization and strain was lost after cycling 10^6 times at 5 kV mm^{-1} of bipolar field (5 Hz), as shown in Figures 4(c) and 4(d).

In conclusion, lead-free KBNFT9 has been shown as a monolithic ceramic and as an MLA to not only exhibit temperature stable and fatigue resistant properties superior to all other comparable lead-free materials but also to commercial PZT formulations.

A.K. and F.H. acknowledge Abdul Wali Khan University Mardan and NED University of Engineering and Technology, respectively, for Ph.D. studentships. All authors acknowledge the financial support from the Sustainability and Substitution of Functional Materials and Devices EPSRC grant (EP/L017563/1).

[1]W. Jo, R. Dittmer, M. Acosta, J. Zang, C. Groh, E. Sapper, K. Wang, and J. Rödel, J. Electroceram. **29**, 71 (2012).
[2]T. Stevenson, D. G. Martin, P. I. Cowin, A. Blumfield, A. J. Bell, T. P. Comyn, and P. M. Weaver, J. Mater. Sci. Mater. Electron. **26**, 9256 (2015).
[3]R. Müller-Fiedler and V. Knoblauch, Microelectron. Reliab. **43**, 1085 (2003).
[4]D. Damjanovic, N. Klein, J. Li, and V. Porokhonskyy, Funct. Mater. Lett. **3**, 5 (2010).
[5]K. Uchino, *Piezoelectric Actuators and Ultrasonic Motors* (Springer US, 1997).
[6]C. Galassi, M. Dinescu, K. Uchno, and M. Sayer, *Piezoelectric Materials: Advances in Science, Technology and Applications* (Springer Netherlands, 2000).
[7]D. C. Lupascu, E. Aulbach, and J. Rödel, J. Appl. Phys. **93**, 5551 (2003).
[8]N. Balke, D. C. Lupascu, T. Granzow, and J. Rödel, J. Am. Ceram. Soc. **90**, 1081 (2007).
[9]C. Verdier, D. C. Lupascu, and J. Rödel, Appl. Phys. Lett. **81**, 2596 (2002).
[10]J. Rödel, K. G. Webber, R. Dittmer, W. Jo, M. Kimura, and D. Damjanovic, J. Eur. Ceram. Soc. **35**, 1659 (2015).
[11]W. Liu and X. Ren, Phys. Rev. Lett. **103**, 257602 (2009).
[12]E. K. Akdogan, K. Kerman, M. Abazari, and A. Safari, Appl. Phys. Lett. **92**, 112908 (2008).
[13]E. Hollenstein, D. Damjanovic, and N. Setter, J. Eur. Ceram. Soc. **27**, 4093 (2007).
[14]S. Zhang, A. B. Kounga, E. Aulbach, W. Jo, T. Granzow, H. Ehrenberg, and J. Rödel, J. Appl. Phys. **103**, 034108 (2008).
[15]Y. Hiruma, R. Aoyagi, H. Nagata, and T. Takenaka, Jpn. J. Appl. Phys., Part 1 **44**, 5040 (2005).
[16]G. A. Smolenskii and A. I. Agranovskaya, Sov. Phys.-Solid State **1**, 1429 (1959).
[17]H. Matsuo, Y. Noguchi, M. Miyayama, M. Suzuki, A. Watanabe, S. Sasabe, T. Ozaki, S. Mori, S. Torii, and T. Kamiyama, J. Appl. Phys. **108**, 104103 (2010).
[18]J. M. Kim, Y. S. Sung, J. H. Cho, T. K. Song, M. H. Kim, H. H. Chong, T. G. Park, D. Do, and S. S. Kim, Ferroelectrics **404**, 88 (2010).
[19]M. I. Morozov, M.-A. Einarsrud, and T. Grande, Appl. Phys. Lett. **101**, 252904 (2012).
[20]M. I. Morozov, M.-A. Einarsrud, T. Grande, and D. Damjanovic, Ferroelectrics **439**, 88 (2012).
[21]D. C. Arnold, K. S. Knight, F. D. Morrison, and P. Lightfoot, Phys. Rev. Lett. **102**, 027602 (2009).

[22]K. Kalantari, I. Sterianou, S. Karimi, M. C. Ferrarelli, S. Miao, D. C. Sinclair, and I. M. Reaney, Adv. Funct. Mater. **21**, 3737 (2011).
[23]X. Qi, J. Dho, R. Tomov, M. G. Blamire, and J. L. MacManus-Driscoll, Appl. Phys. Lett. **86**, 62903 (2005).
[24]A. Khesro, R. Boston, I. Sterianou, D. C. Sinclair, and I. M. Reaney, J. Appl. Phys. **119**, 054101 (2016).
[25]D. J. Cumming, T. Sebastian, I. Sterianou, J. Rödel, and I. M. Reaney, Mater. Technol. **28**, 247 (2013).
[26]J. Yang, Y. Hou, C. Wang, M. Zhu, and H. Yan, Appl. Phys. Lett. **91**, 23118 (2007).
[27]Z. F. Li, C. L. Wang, W. L. Zhong, J. C. Li, and M. L. Zhao, J. Appl. Phys. **94**, 2548 (2003).
[28]J. Kuwata, K. Uchino, and S. Nomura, Jpn. J. Appl. Phys., Part 1 **19**, 2099 (1980).
[29]Y. Saito, H. Takao, T. Tani, T. Nonoyama, K. Takatori, T. Homma, T. Nagaya, and M. Nakamura, Nature **432**, 84 (2004).
[30]D. Wang, Y. Fotinich, and G. P. Carman, J. Appl. Phys. **83**, 5342 (1998).
[31]M. Acosta, *Strain Mechanisms in Lead-Free Ferroelectrics for Actuators* (Technische Universität Darmstadt, 2015).